INFLUENCE OF THE FORMING PROCESS ON THE CORROSION RESISTENCE OF AA3103 ALUMINIUM PIPES

Chiara Schmid, professore, Dipartimento di Ingegneria dei Materiali e Chimica Applicata Università di Trieste, Via A. Valerio 34127 Trieste
Giuseppe Pecoraro, ingegnere, collaboratore esterno (UD)
Nicola Scuor, ricercatore, Dipartimento di Ingegneria dei Materiali e Chimica Applicata Università di Trieste, Via A. Valerio 34127 Trieste

1. Introduction

Weight reduction and ensuing increased fuel-efficiency represents some of the main aims of the automobile industry. Lightweight aluminium alloys have been newly developed and have gradually resulted in increased usage in automobile applications.
In the industrial sector linked to the automobile market there is an increasing demand of corrosion resistant aluminium products. Heat exchanger and radiator tubes represent an important application field.
Aluminium and aluminium alloys are actually active materials from a corrosion point of view; fortunately they can develop an insulating film in the ambient atmosphere as a result of their natural tendency for direct oxidation with atmospheric oxygen under normal conditions. The stability of the surface oxide formed on these materials and its protective nature represent a major field of research. [1]
Aggressive anions, like Cl^-, lead to increased corrosion rates and film breakdown; in these solutions, pitting corrosion takes place. [2]
In the present essay we investigate the influence of the forming methods on the corrosion resistance of a widely used aluminium alloy, AA3103.
The alloy Al-Mn (AA3103) is one of the aluminium alloys that resist more to atmospheric corrosion and therefore it is widely used in the car manufacturer industry. [1]
The SWAAT standardised test is employed to highlight the tubes' resistance to corrosion. As far as duration (resistance) for automobile tubes is concerned, they range from values of minimum 22 days (528 h) to values of minimum 40 days (960 h) and this for a continuous increase of the quality standards.

2. Materials

We have considered commercial tubes in Al-Mn alloy of four different companies used in the car manufacturer industry. Each of these four types is characterised by a different forming process or, in one case, by a different composition. In fact three tubes are in nominal alloy AA3103, while another has a non-standard composition (long life alloy). The composition of the AA3103 alloy as UNI 9003 is reported in Tab.1. The samples identification is reported in Tab.2.

Tab.1 Composition of the AA3103 alloy (UNI 9003)

Si	Fe	Cu	Mn	Mg	Cr	Zn	Ti + Zr	Other impurities		Al
max	max	max		max	max	max	max	each max	total max	
0.50	0.7	0.10	0.9 ÷ 1.5	0.30	0.10	0.20	0.10	0.05	0.15	rem

Tab.2 Samples identification.

Identification n°	Forming process	alloy
1	Billet Conventional direct extrusion, cold-draw, thermal treatment	AA3103
2	Conventional direct extrusion	Long life alloy
3	Conventional direct extrusion	AA3103
4	Continuous extrusion	AA3103

3. Experimental methods

Pieces of tubes of a similar length (300 mm ca.), has been welded at one end and closed with a plastic sealing at the other one and finally they have been subjected to a SWAAT test

-The Sea Water Acetic Acid Test (SWAAT) – ASTM G85
This test consist in putting the cleaned sample in a salt spray (fog) chamber; the temperature is maintained at 50°C; the solution is a synthetic sea salt solution in accordance with specification D1141, acidified by glacial acetic acid to a pH between 2.8 and 3.0; the spray cycle is: 30 min spray followed by 90 min soak at above 98% relative humidity. Periodically (about 100 hours) the tubes are pneumatically tested to verify their integrity. This test indicates if there is a leak; when this happens the part is considered to be failed (time of failure).

After the above-mentioned test, the surface and section of the various samples is analysed visually and with the optical microscope.
Fluorescence and Raman spectroscopy as well as EDX investigations have been carried out in order to identify the surface's deposits after SWAAT.
Samples sections were cut from the tubes after SWAAT, incorporated in resin, mechanically polished and then an anodic electrolytic oxidation in HBF_4 solution as medium for the micro observation was carried out; macro etching with Tucker solution on external surfaces of the as received tubes was also done.

4. Results

-Time of failure
As previously said, the aluminium alloy undergoes pitting corrosion if there is presence of chlorine ions; the aim of the SWAAT is to accelerate the pit formation and growth using i) an acidic ambient though not directly aggressive (acetic acid), ii) chlorine ions depassivation effect (NaCl), iii) oxygen (cyclic test) and iv) temperature effect (50°C).

In Tab.3 the timing of failure for the samples, as well as their dimensions (external diameter, Φ and thickness, s) are reported.

Tab.3 Samples identity number, dimensions and time of failure under SWAAT.

Id. N°	Φ x t [mm]	Time of failure [h]					
		240	600	700	815	1150	1320
1.a	16x1.24	ok	ok	**KO**			
1.b	18x1	ok	**KO**				
2.a	14x1.24	ok	ok	ok	ok	**KO**	
3.a	15x1	ok	**KO**				
3.b	18x1	**KO**					
4.a	10x0.85	ok	ok	ok	**KO**		
4.b	20x1	ok	ok	ok	ok	ok	**Did not fail**

-Surface conditions
The surfaces conditions are visible in figures 1 to 4.

Fig.1 picture of the 1.a tube in two magnifications.

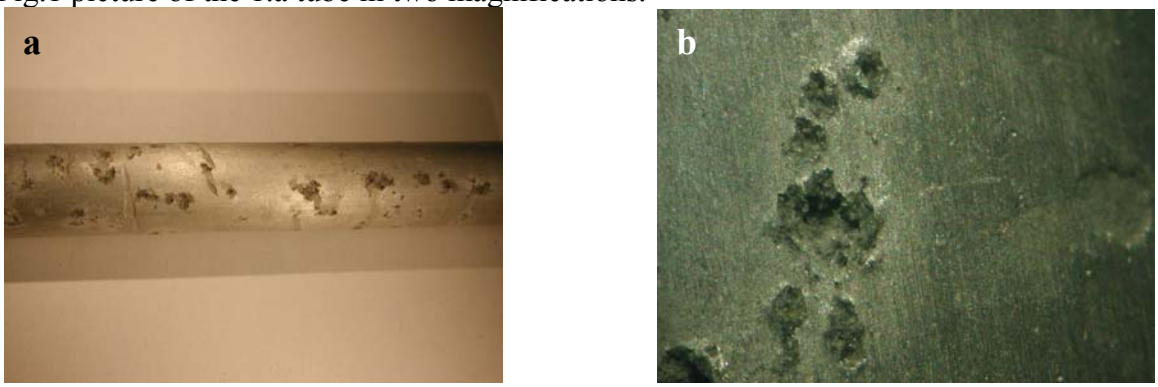

Fig.2 Picture of the 2.a tube in two magnifications.

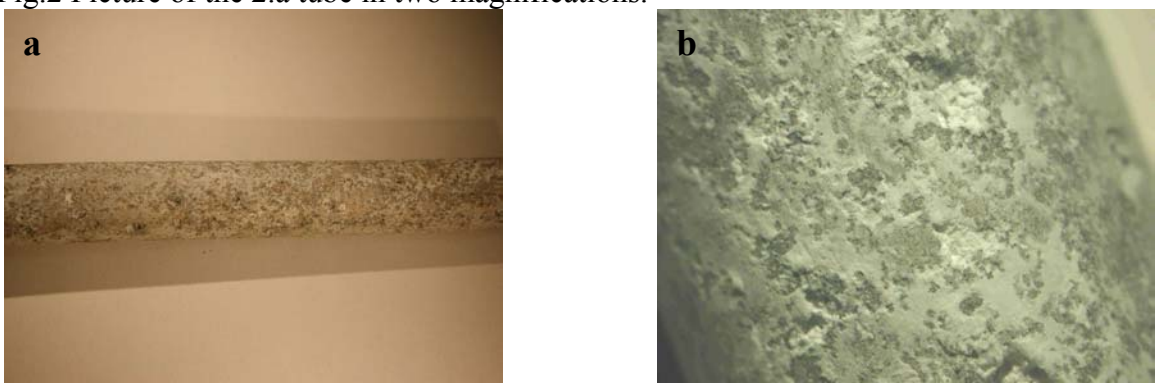

Fig.3 picture of the 3.a tube in two magnifications.

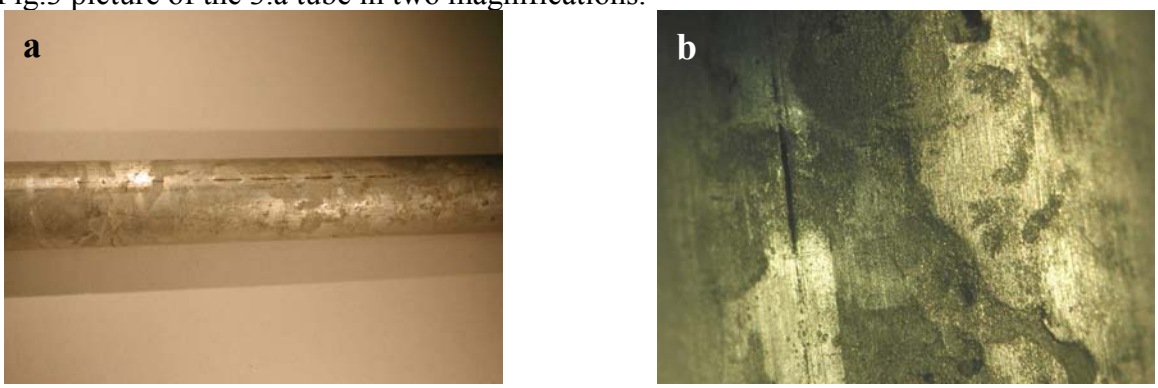

Fig.4 Picture of the 4.b tube in two magnifications.

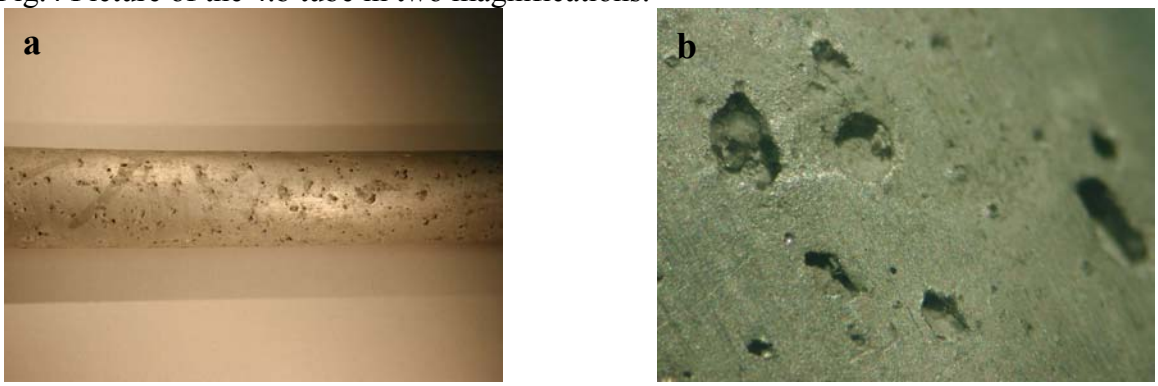

-Pit density

The 1.a, 2.a, 3.a and 4.b samples have been optically examined and the surfaces pits on a similar area counted; the pit density vs. the time of failure is reported in Graph.1.

Graph.1 Pit density vs. time of failure.

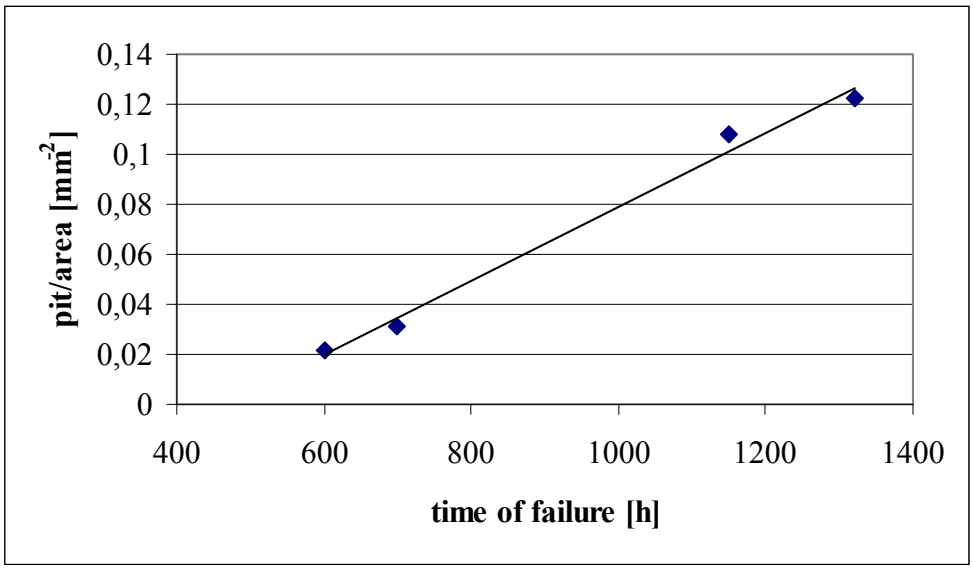

-Pit morphology

Sections of the tubes have been carried out next to surface damages; the pits appearance is visible in Fig. 5-8.

Fig.5 Picture of a 1.a tube section in two magnifications.

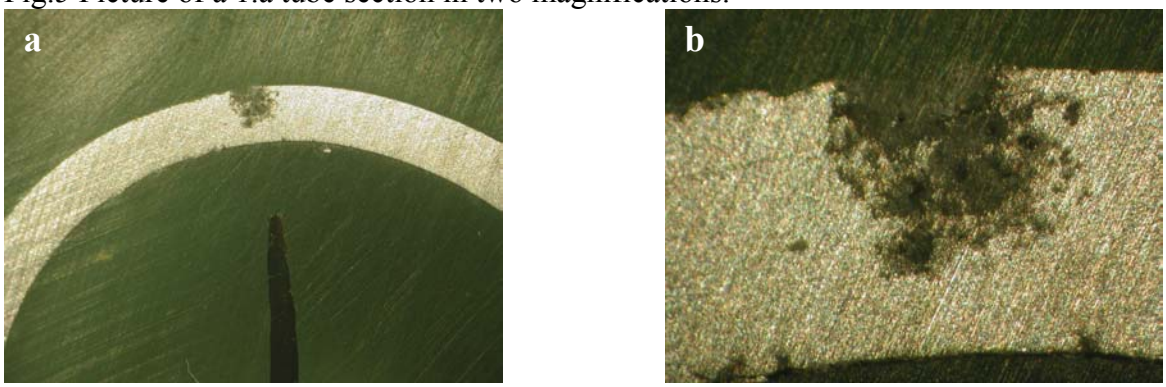

Fig.6 Picture of a 2.a tube section in two magnifications.

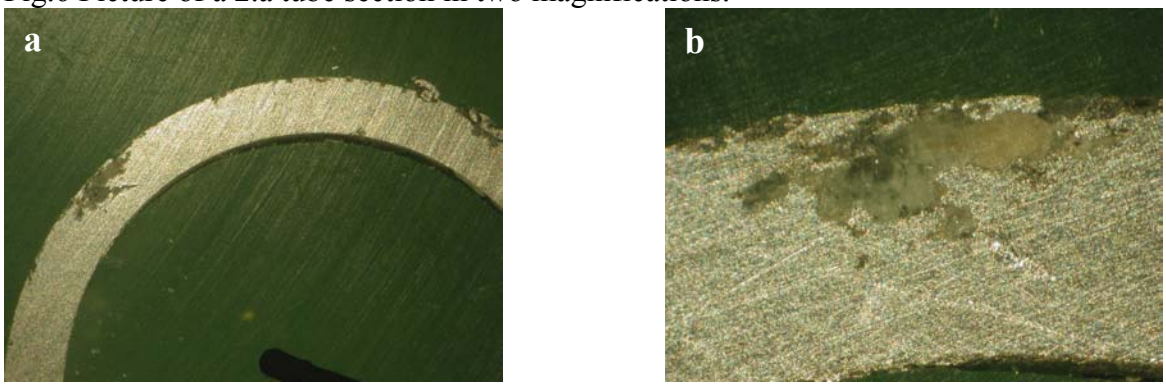

Fig.7 Picture of a 3.a tube section in two magnifications.

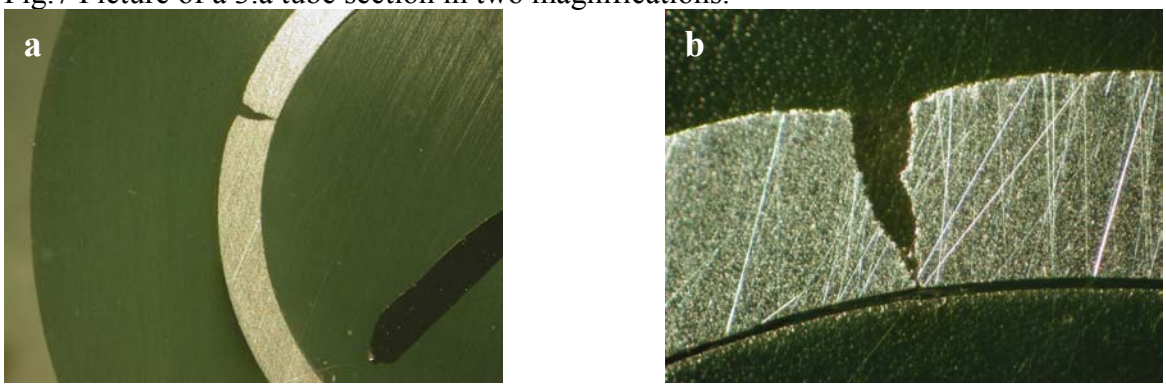

Fig.8 Picture of a 4.b tube section in two magnifications.

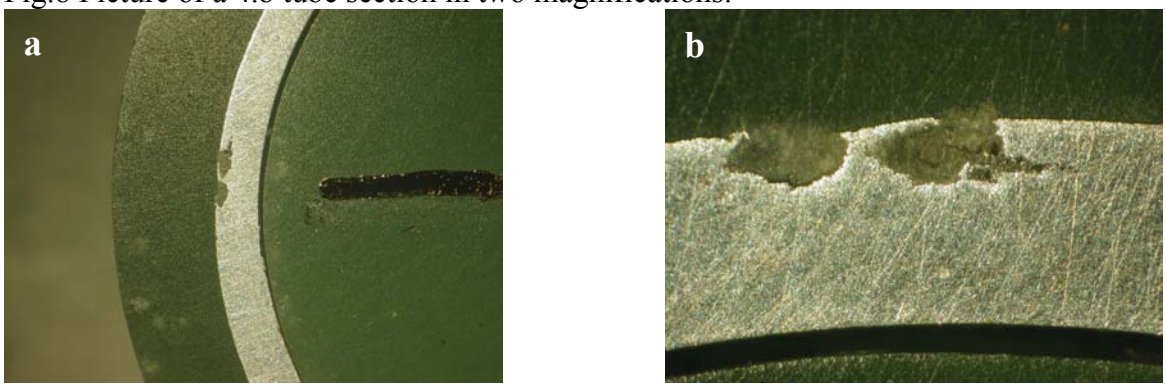

-External (surface) macrostructure

On cleaned tubes a macro etching with Tucker solution was made. Fig. 9-12 show images (same enlargement) concerning the 4 samples.

It is notable that samples 2 and 3 are those with finer grain, while samples 1 and 4 have a comparable larger dimension. In the samples 1, 2 and 3 the grains size is homogeneous on the whole circumference, while sample 4 shows longitudinal zones with thicker grain (the one shown in Fig.12) alternated with others with very fine grain. Moreover in sample 1 the presence of elongated grains is evident (the tubes shown in the pictures have the same orientation).

Fig.9 Picture of the surface macrograph of the n°1 sample.

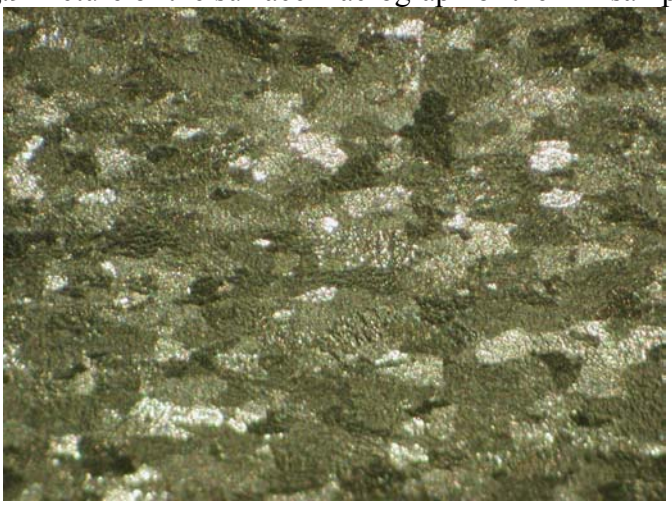

Fig.10 Picture of the surface macrograph of the n°2 sample.

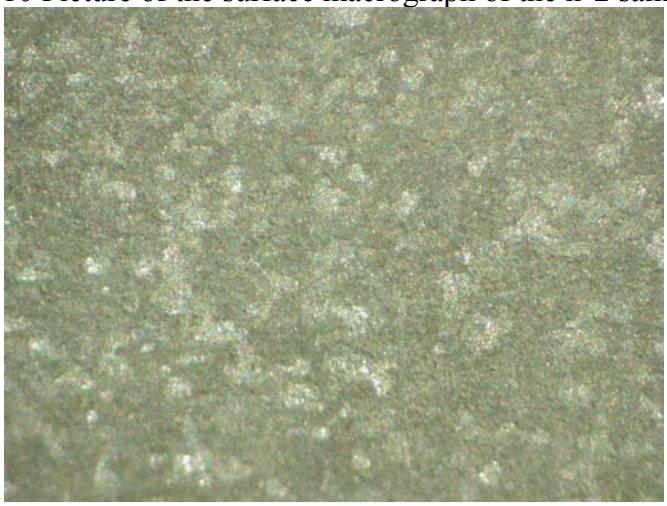

Fig.11 Picture of the surface macrograph of the n°3 sample.

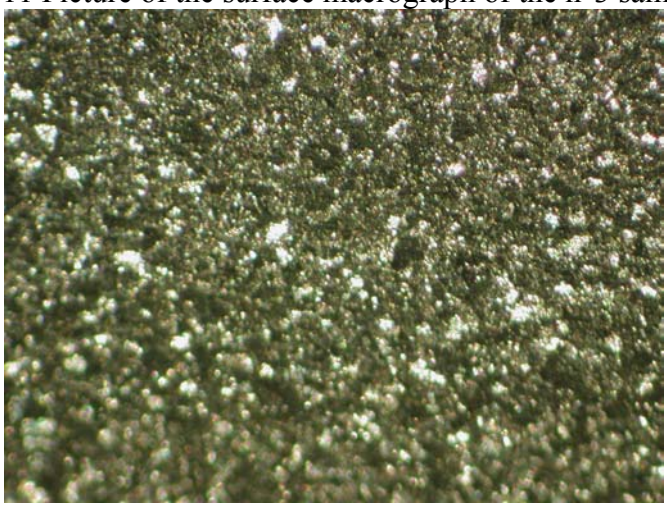

Fig.12 Picture of the surface macrograph of the n°4 sample.

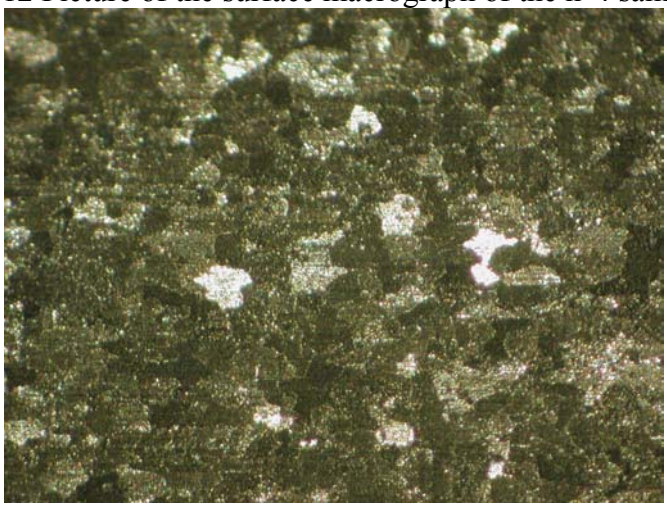

-Identification of deposits

In each of the 4 cases, the EDX analysis highlighted the presence of Al and O in such a quantity to affirm that principally there is formation of alumina (Al_2O_3). Furthermore there is the presence (in a variable quantity for the 4 samples) also of chlorine, localised principally at the bottom of the pits.

For example in Graph.2 is reported the sample n°2 EDX spectrum.

Graph.2 EDX spectrum of the deposit present in the pit for sample n°2.

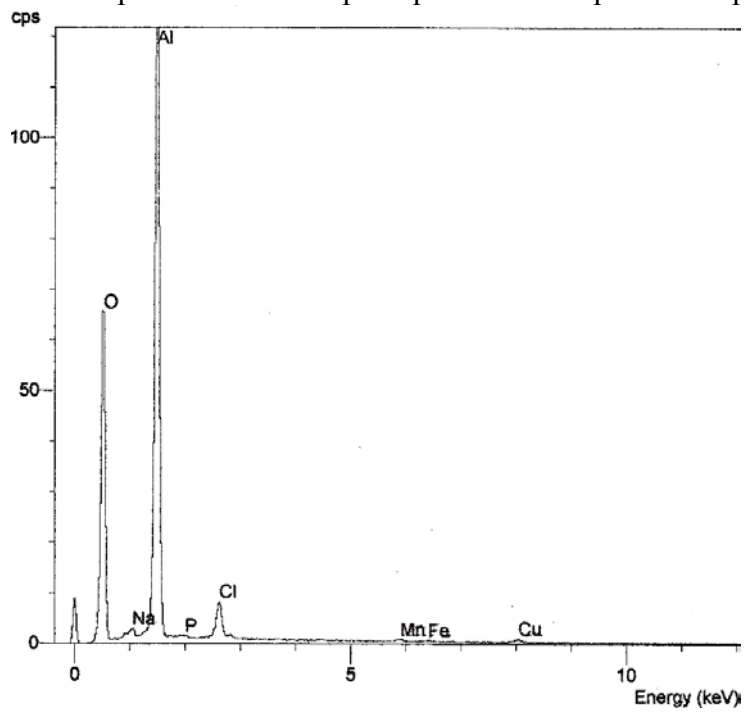

Effectively, fluorescence spectroscopy shows that crystallized alumina is only present in sample 3 and 4, while in sample 2 Raman spectroscopic shows the presence of also another phase (probably a mixed oxy-chloride).

-Section microstructure

Some sections of the four samples after SWAAT have been polished and electrolytically etched in HBF_4 medium. The observation was done in polarized light. The micrographs are reported in Fig.13-16.

Fig.13 Picture of a etched section of sample n°1.

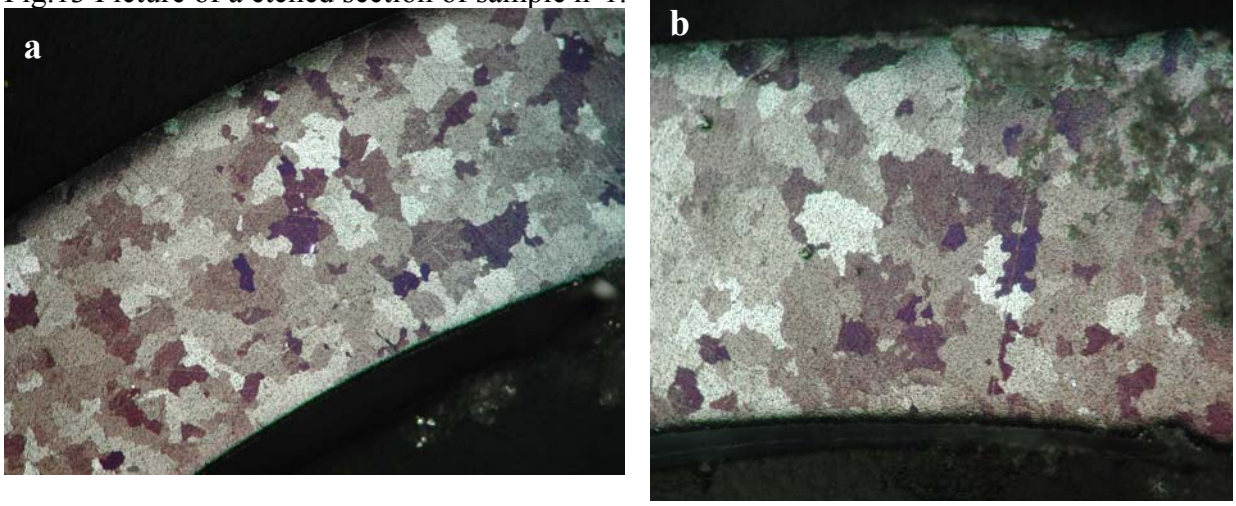

Fig.14 Picture of a etched section of sample n°2.

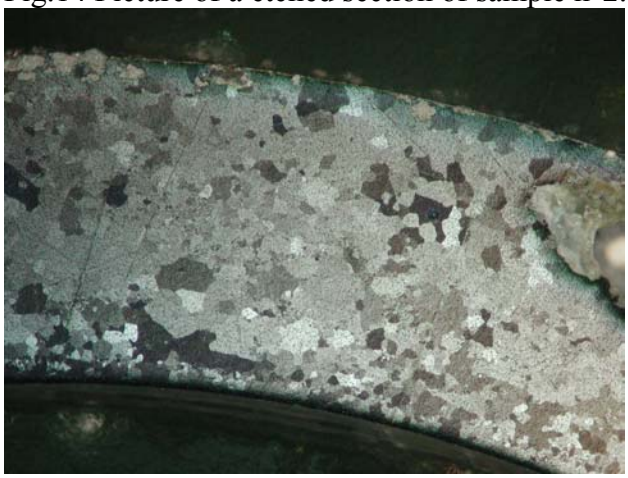

Fig.15 Picture of a etched section of sample n°3.

Fig.16 Pictures of a etched section of sample n°4.

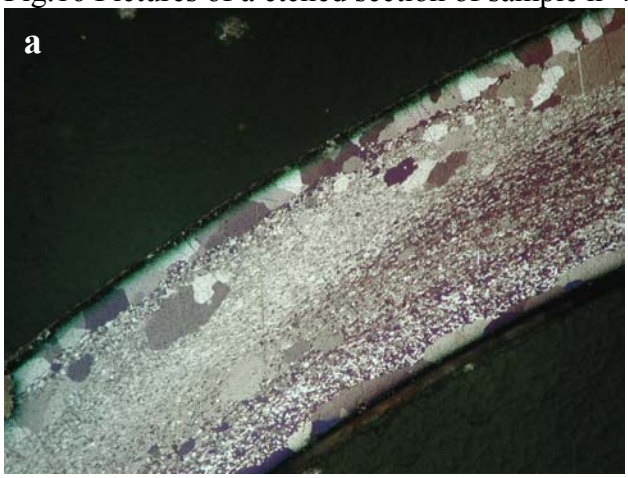

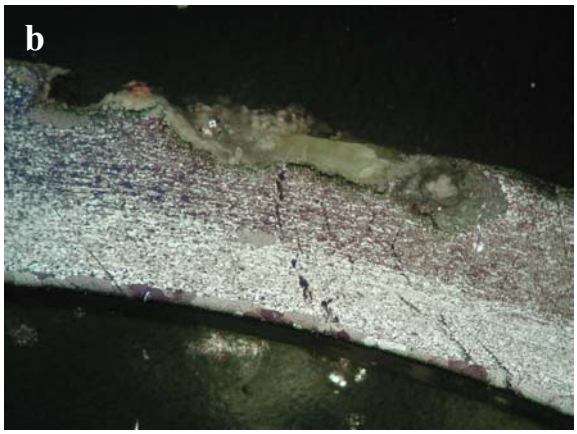

Image analysis on the micrographs has permitted to determine the mean grain size, reported in Tab.4.

Tab.4 Image analysis results for the 4 samples.

Id. n°		GSmean [μm]	Standard deviation	Number of grains	Gsmin [μm]	Gsmax [μm]
1		110	52	273	26	281
2		71	37	284	17	251
3		46	13	274	17	90
4	skin	137	83	284	40	434
	core	11	4	518	5	22

5. Discussion and conclusion

All the samples undergo pitting corrosion attack.
Examining the pit density (Graph.1) it can be noted that samples 1 and 3, which have few pits, fail before samples 2 and 4, which, on the other hand, have developed numerous pits.
The most obvious explanation of this fact is that few pits have a faster kinetic of growth (higher ratio between cathodic and anodic area) if compared to that of several pits (lower ratio Acat/Aan).
A reasonable starting assumption may be that the pit density is correlated with the exposed area, i.e. it is dependent on the external tube diameter. In fact, the sample 4.b has the larger diameter and the grater pit density; samples 1.a and 3.a have behaviour that match too with the initial statement (higher diameter = higher pit density).
On the contrary, the pit density for the sample 2.a, that has the diameter lower than samples 1.a and 3.a, is higher. In this case however the alloy composition is different (long life alloy): EDX analysis shows that it has a higher quantity of iron respect the AA3103 nominal composition; the presence of Fe causes surface depolarisation and consequently a higher density of localized corrosion.
Comparing samples with same composition (see Tab.3), sample 4.a, that present the minor diameter (10 mm) has a time of failure higher than that of samples n°1 and n°3 that instead have bigger diameter; it has also to deduce that exposed area is not the only critical factor in the corrosion resistance.
Comparing samples with same processing (samples n°2 and n°3) it can be seen that the composition heavily influences corrosion resistance (the long life alloy seems to be more resistant than AA3103); it has to be said however that sample n°3 failed mostly along the seams (see Fig.3). Anyway, comparing the pit morphology of sample n°2 (Fig.14) with that of sample n°3 but out of seam zone (Fig.15), it can be seen that they are similar, being the depth of sample n°3 higher (in less time).
Comparing the different forming processes (samples n°1, n°3 and n°4), taking also in account the observation on samples n°3 reported above, it can be noted that conventional extrusion (sample n°3) has worse behaviour than the tube cold-down and thermal treated (sample n°1), that is worse than the continuously extruded one (sample n°4).
When considering the microstructure of the four samples (Fig.13-16), substantial difference can immediately be noted: the samples 1, 2 and 3 have roughly a homogeneous grain size (GS) on the whole section, whereas in sample n°4 bands with different grain sizes are clearly visible.

The sample n°1 has the higher GS (110 μm), due to the thermal treatment (Fig.13a); the pit (Fig.13b) can grows without any hindrance, propagating through the grains and the grain boundaries (see also Fig.5b).
The sample n°2 (Fig.14) has a less homogeneous microstructure, having a bimodal GS distribution within the section (GSmean is 71 μm); the pit grows well defined in crater shape.
The sample n°3 presents a very homogeneous microstructure with small GS (46 μm); the pit grows well defined in crater shape if it is located out the seam zone (Fig.15), the perforating one in the seam zone is shown in Fig.7b.
In the sample n°4 instead two zone with big GS (137μm) are distinguishable (internal and external borders, with mean thickness of 72 and 149 μm respectively), while the core has a very fine GS (11 μm).
This *organized* unhomogeneity is probably due to the forming process that produces temperature and stress gradients along the thickness of the tube [3-10] capable of a recrystallization process in the core zone [11-14].
In Fig.16b it can be note how the pit propagation is slowed down in the recrystallized band (the depth of the pit is smaller than that in the other samples, although the time of exposition is longer); in general, after their formation, the pits grow parallel the surface, showing systematically a flat bottom (see Fig.4b and 8b); in some case there is also blisters formation, as reported in Fig.17.

Fig.17 picture of a blister on the n°4 sample surface.

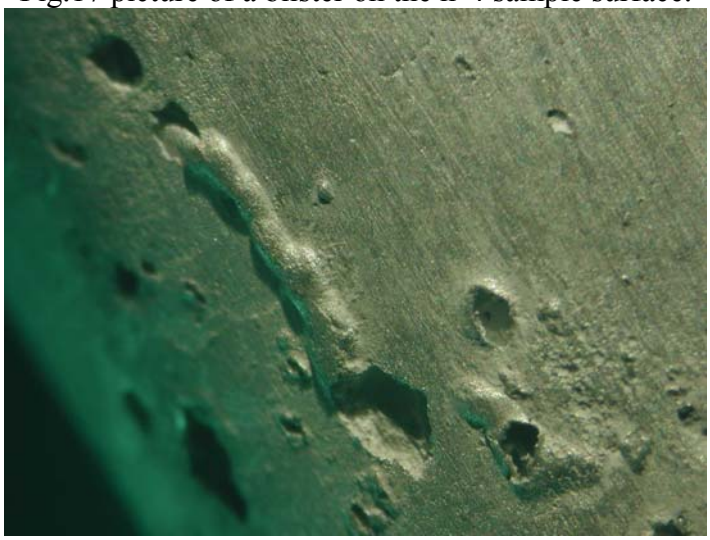

The conclusions of the present paper can be summarized as follow:

- the SWAAT is used to accelerate the corrosion for aluminium alloy; corrosion takes place as pitting;
- the time of failure depends directly on the exposed area, that is on the surface pit density;
- the time of failure depends on the tortuosity of the pit's path, and whether or not it is parallel to the surface;
- the kinetic and the path of the pit growth are determined by the microstructure;
- the various formation processes of the tubes yield different microstructures;
- continuous extrusion induces a recrystallization effect (that is a skin effect) capable of opposing pit propagation along the thickness, making pits to deviate under skin (blistering) and thus increasing the time of failure.

References

[1] Hollingsworth E.H., Hunsicker H.Y., “Corrosion of aluminium and aluminium alloys”, in Metal Handbook 9th Ed. Vol.13 Corrosion 583-609 (1987)

[2] Reboul M.C., Warner T.J., Mayet H., Baroux B., “A ten step mechanism for the pitting corrosion of aluminium alloys”, Corrosion Review, 15, 3-4, 471-496 (1997)

[3] Mingdian L., Baoyun S., “Study of the velocity field and the stress field in the Conform”, Adv. Tech. Plast. (1993).

[4] Kim Y.H., Cho J.R., Kim K.S., Jeong H.S, Yoon S.S., “A study of the application of upper bound method to the Conform process”, J. Mat. Proc. Tech. 97, 153-157 (2000).

[5] Sinha U., Chia E.H., “Metallurgical considerations for quality improvements of Conform aluminium products”, Aluminium Association (1998).

[6] Lu J., Saluja N., Riviere A.L., Zhou Y., "Computer modeling of the continuous forming extrusion process of AA6061 alloy", J. Mat. Proc. Tech. 79, 200-212 (1998).

[7] Yinghong P., Tioyong Z., Dashu P., Xueyu R., "Simulation of the CONFORM process: numerical and experimental methods", Adv. Tech. Plasticity (1993).

[8] Kim Y.H., Cho J.R., Kim K.S., Jeong H.S, Yoon S.S., “A study on optimal design for Conform process”, J. Mat. Proc. Tech.80-81, 671-675 (1998).

[9] Yinghong P., Tieyong Z., Dashu P., Xueyu R., “Simulation of the Conform process: numerical and experimental methods”, Adv. Tech. Plast. (1993).

[10] Cho J.R., Jeong H.S., "Parametric investigation on the surface defect occurrence in CONFORM process by the finite element method", J. Mat. Proc. Tech. 104, 236-243 (2000).

[11] Vatne H.E., Engler O., Nes E., "Influence of particles on recrystallisation texture and microstructures of aluminium alloy 3103", Mat. Sc.tech. 13, 93-102 (1997).

[12] Doherty R.D. et al., "Current issue in recrystallization: a review", Mat. Sc. Eng A238, 219-274 (1997)

[13] Doherty R.D., Szpunar J.A., "Kinetics of sub-grain coalescence – a reconsideration of the theory", Acta Met. 32, 1789-1798 (1984).

[14] Engler O., Yang P., Kong X.W., "On the formation of recrystallization textures in binary Al-1.3%Mn investigated by means of local texture analysis", Acta Mat. 44, 3349-3369 (1996).